

# High Surface-to-Volume Ratio ZnO Microberets: Low Temperature Synthesis, Characterization, and Photoluminescence

Hongbing Lu, Lei Liao, Jinchai Li,\* Duofa Wang, Hui He, Qiang Fu, Lei Xu, and Yu Tian

Department of Physics and Key Laboratory of Acoustic and Photonic Materials and Devices,  
Ministry of Education, Wuhan University, Wuhan 430072, People's Republic of China

Received: June 29, 2006; In Final Form: September 15, 2006

Novel hollow ZnO microstructures and ZnO microberets (ZMBs) with nanowires grown vertically on both the inner and outer surfaces of beret shells were synthesized on Si(100) substrates by simple thermal evaporation of pure zinc powder without any catalyst or template material at a relative low temperature of 490 °C. XRD, SAED, and HRTEM patterns show that the nanowires and shells of ZMBs are single-crystalline wurtzite structures. The growth mechanism of ZMBs is discussed in detail. The formation of these hollow microstructures depends on the optimum starting time of air introduction. It is a good way to grow well-aligned nanowires by using a nanoscale rough ZnO surface to realize a “self-catalyzed” vapor–liquid–solid process. The photoluminescence spectrum reveals a strong green emission related to the high surface-to-volume ratio of ZMBs. These types of special hollow high surface area structural ZMBs may find potential applications in functional architectural composite materials, solar cell photoanodes, and nanooptoelectronic devices.

## 1. Introduction

Over the past few years, much effort has gone into the production of various ZnO nanostructures of specific morphologies, including nanowires, rods, belts, pencils,<sup>1</sup> and screws,<sup>2</sup> which are important in various applications such as light-emitting diodes,<sup>3</sup> gas sensors,<sup>4</sup> nanocantilevers,<sup>5</sup> transducers, and biomedical sciences.<sup>6</sup> Specific hollow nano/microstructures are attracting considerable interest because of their lower densities and higher surface areas compared with their bulk counterparts. They therefore may find potential applications in filters, coatings, capsule agents for drug delivery, templates for functional architectural composite materials,<sup>7</sup> photocatalysis,<sup>8</sup> and photoanodes of solar cells.<sup>9</sup>

Several methods have been developed for the preparation of submicrometer hollow spheres of inorganic materials, such as liquid droplets,<sup>10</sup> polymer beads,<sup>7</sup> and colloidal templates.<sup>11</sup> However, all of the above methods require additional template materials to build sphere architectures, and the template needs to be removed later. Recently, Gao reported a method using Sn catalysis without a template material to prepare hollow microspheres where the mesoporous ZnO shells were obtained by the reactive evaporation of the mixed ZnO, SnO<sub>2</sub>, and graphite powders at high temperature (1150 °C).<sup>12</sup> In this paper, we report the preparation of hollow ZnO microstructures—ZnO microberets (ZMBs) with ZnO nanowires grown vertically on both the inner and outer surfaces of ZnO beret shells. The ZMBs are synthesized by simple thermal evaporation of pure zinc powder without using any catalyst or template at a relatively low temperature of 490 °C. The growth mechanism of ZMBs will be discussed in detail.

The morphology and crystalline structure of ZMBs were characterized by Sirion FEG scanning electron microscopy (SEM), D8 advanced X-ray diffraction (XRD), JEOL JEM 2010

transmission electron microscopy (TEM), and high-resolution transmission electron microscopy (HRTEM). The room-temperature photoluminescence (PL) spectra were measured using a He–Cd laser as the excitation source (325 nm).

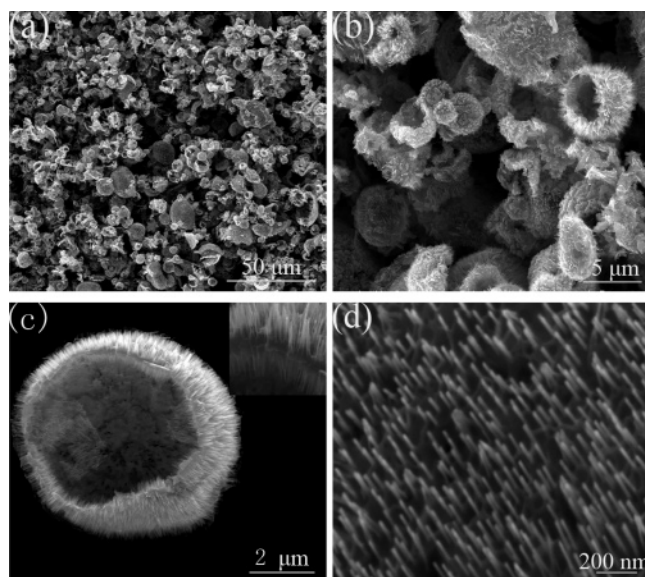
## 2. Experimental Section

Zinc powder (99.99% purity) was placed on a quartz boat that was inserted into the center of a horizontal tube furnace. Si(100) p-type substrates were etched by hydrofluoric acid and cleaned by the action of deionized water and ethanol. The cleaned Si substrates were located downstream at a position where the distance to the Zn source is about 8 mm. The system was first pumped to a base vapor pressure of about 3 Pa, and then argon was introduced into the system with a flow rate of 50 sccm as a carrier gas. Afterward, the tube was heated to 490 °C at a rate of 15 °C/min. When the temperature reached 460 °C, a flow of 40 sccm of air was then added to the quartz tube. The synthesis process was carried out under the pressure of 20 Pa at 490 °C and lasted for about 30 min. The gas flows were cut off when the furnace was turned off, and the samples were then naturally cooled at 3 Pa.

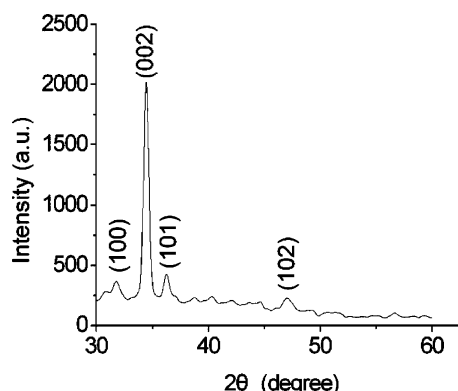
## 3. Results and Discussion

Figure 1 shows the representative SEM images of the obtained samples. Parts a and b (b is a magnification of the image in part a) of Figure 1 display the distribution, size, and morphology of ZMB products. They are distributed over an area of 4 cm<sup>2</sup> × 13 cm<sup>2</sup> uniformly, with slightly different size and morphology. Larger scale production can be achieved by modifying the preparation equipment. Figure 1b clearly shows that the ZMBs are generally ringent and have hollow interiors. Most ZMBs have gaps like those of the microberets, and a few of them have gaps like those of the bucket-cap or bowl-like shapes. The diameters of ZMBs range from 3–8 μm with the majority of them with a diameter of 5 μm. Figure 1c shows an individual ZnO microberet. One may observe that the ZnO microberet is

\* Corresponding author. Department of Physics, Wuhan University.  
Tel: +86-27-6875-2567. Fax: +86-27-6875-2569. E-mail: jcli@acc-lab.whu.edu.cn.



**Figure 1.** SEM images of ZMBs with nanowires: (a) a large number of berets; (b) high magnification; (c) an individual beret; inset is magnified image of beret's edge; (d) aligned nanowires grown on the outer surface of beret.



**Figure 2.** XRD pattern of ZMBs on Si(100) substrates.

extraordinarily symmetrical and that nanowires grow on both the inner and outer surfaces of the beret shell. This can be more clearly observed from the Figure 1c inset image, which shows the enlarged picture of the edge of the beret. In the inset image, the bright upside section shows ZnO nanowires grown outward, the dark underside shows ZnO nanowire arrays grown inward, and the middle segment shows the cross section of the ZnO beret shell (a whole beret shell is shown in Figure 4a). Figure 1d represents well-aligned nanowires grown outside the beret. The diameter of the entire body of nanowire is uniform at about 16 nm (according to TEM observations), and the lengths of the nanowires are between 300 and 500 nm with the majority of lengths at around 400 nm.

XRD and TEM were employed to investigate the crystalline structures of the samples. The XRD pattern of the sample is displayed in Figure 2. The diffraction peaks can be well-indexed to the phase-pure, wurtzite hexagonal ZnO. The (002) peak at  $34.3^\circ$  is dominant, indicating that the ZMBs grow along a preferred orientation of the  $c$  axis. A typical HRTEM image of an individual nanowire grown outside the beret is described in Figure 3. It clearly shows that the ZnO nanowires possess a single-crystal structure. Furthermore, the spacing of 0.26 nm between adjacent lattice planes corresponds to the distance of (0002) planes, showing that [0001] is the growth direction of the ZnO nanowires. The inset in Figure 4a presents the image

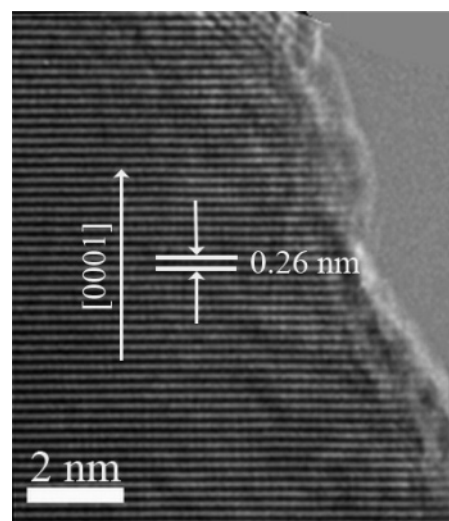


**Figure 3.** HRTEM image of an individual ZnO nanowire.

of a selected area electron diffraction (SAED) taken from the edge area of the gap of the beret shell. The corresponding electron diffraction pattern can be indexed as [0001] zone axis wurtzite ZnO, which reveals that the ZMBs are also single crystal.

To clarify the growth mechanism, a series of SEM images of ZMBs grown at different growth stages are shown in Figure 4. Figure 4a displays the image of a ZnO hollow microshell with a rough surface (the corresponding formation process of this is shown in Figure 5, and the growth mechanism is discussed in succession). From Figure 4a, we can clearly see that there are many small protrusions on the surface of the hollow shell. These kinds of microstructures can be considered as early phases of ZMBs. The presence of small protrusions on the surface of the ZnO hollow sphere shell provides nuclear seeds for the absorption of thermally evaporized Zn atoms, resulting in preferential nucleation for the growth of ZnO nanowires on the protrusions. The SEM image in Figure 4b supports our above deduction, as nanowires have grown sparsely on the beret shell surface and most of them have preferentially formed on the small protrusions. The preferential nucleation and growth of nanowires on the protrusions lead to a divisional growth phenomenon of ZnO nanowires on the surface of the shell, as illustrated in Figure 4d (the magnified image of a ZnO microberet). Along with further growth, the subareas of the nanowires joined each other and gradually folded (Figure 4c), finally bringing on well-proportioned and dense ZnO nanowires over both the inner and outer surfaces of the hollow shell (shown in Figure 4e). Figure 4f exhibits a ZnO hollow sphere with three gaps. Although the images of parts a–e of Figure 4 are not taken from a single ZnO sphere grown in different stages, we believe that they well-illustrate the gradual evolution process of a complete ZnO microberet. Repeated experiments prove that our obtained ZMBs are reproducible. Moreover, we have investigated the formation process of ZMBs by varying the experimental conditions. The results reveal that it is only after the formation of spherical Zn particles that the introduction of air plays an important role in obtaining our ZMBs. When air was introduced before a temperature of  $350^\circ\text{C}$  was reached, nanowires, nanorods, or needlelike nanostructures were obtained, but no ZMBs were found. Therefore, we believe that the starting time of air addition has been the main influence on the formation of ZMBs in our experiments. Based on the above characterizations and description, the growth mechanism is discussed in

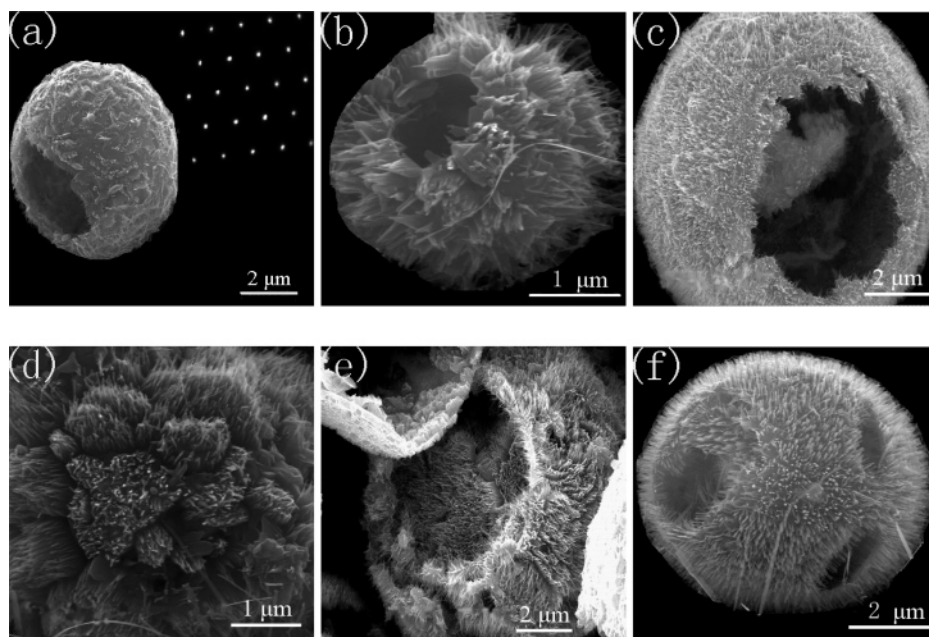


**Figure 4.** SEM images of ZMBs grown at different stages: (a) ZnO hollow sphere shell with rough surface; inset is SAED pattern of gap's edge area; (b) hollow sphere with nanowires grown sparsely on the surface; (c) hollow sphere with relatively thick nanowires; (d) magnified image of ZnO nanowires grown divisionally on rough surface; (e) a complete ZnO beret with dense nanowires on the inner and outer surfaces; (f) a hollow sphere with nanowires and three gaps.

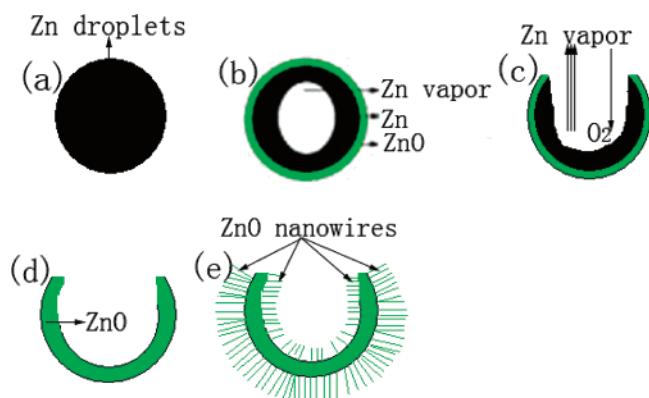


**Figure 5.** Schematic illustration of the formation process of ZMBs.

detail as follows, and the corresponding schematic illustrations of the formation process are shown in Figure 5.

First, Zn droplets assemble into sphere-shaped particles due to the supersaturation of Zn vapor. This is also confirmed by Gao's report.<sup>12</sup> According to their perspective, the shapes of liquid Zn droplets should be spherical when the temperature approaches the melting point of Zn (around 420 °C) and beyond. In our experiment, the Zn vapor is first condensed on the Si substrate and forms liquid droplets. Along with the ascension of temperature, a mass of Zn liquid droplets rapidly diffuse and solidify into spherical Zn particles (shown in Figure 5a).

Then, the spherical Zn particles are transformed into hollow ZnO spheres due to quick oxidation of the Zn particle surfaces and the sublimation of the Zn ration within particles after the introduction of air to the reactive chamber. When air is introduced at 460 °C, the surfaces of spherical Zn particles are immediately oxidized into ZnO films, and film thickness gradually increases with the rising temperature. Meanwhile, the Zn enclosed inside the ZnO thin film layer begins to sublime because the environmental temperature is over the melting point of Zn. However, the outer ZnO film cannot be melted due to its high melting point (around 1 975 °C). The Zn steam is thus

encaged by the outer ZnO film and accumulates, inducing a higher pressure inside the ZnO sphere shell than that outside (shown in Figure 5b). Simultaneously, the ZnO shells become thicker by oxidation. As a result, the weak part of the sphere shell is breached when the vapor pressure becomes greater than that which the local ZnO shell can sustain (shown in Figure 5c). Subsequently, oxygen diffuses inward, and a complete ZnO hollow sphere shell is formed by further oxidation of the inner sphere walls (displayed in Figure 5d). Sometimes there may be several gaps formed on a ZnO hollow sphere shell because several parts are simultaneously broken, as shown in Figure 4f. With regard to the origin of the sphere gaps, our viewpoint is different from the previous reports of others. According to Gao's report, the gaps of their ZnO cages originated from the Zn–ZnO lattice mismatch, and then the Zn inside sublimates through the gaps. In our case, perhaps the lattice mismatch has some influence on the local outbursts, but it is not dominant.

Eventually, ZnO nanowires grow vertically on both the inner and outer surfaces of spherical microshells (as shown in Figure 5e). In the conventional vapor–liquid–solid (VLS) process, the growth of nanowires occurs through the catalyst droplets at the ends of nanowires. Metal catalysts and metal catalyst alloy droplets at the ends of nanowires are the main characteristics of that kind of process. In our study, no metal catalyst or metal catalyst alloy is used in the reaction; thus, the growth mechanism cannot be a conventional VLS, and it is most likely governed by a “self-catalyzed” VLS process. The rough inner and outer surfaces of ZnO shells may offer a nucleating center to facilitate the condensation of Zn atoms. Zn atoms condense and form a large quantity of liquid droplets on both surfaces of the sphere shell. Then the Zn droplets react with O<sub>2</sub> to form ZnO. Therefore, Zn droplets not only serve as the reactant but also provide an energetically favored site for the adsorption of oxygen. Due to the perfect lattice match, the nuclei are formed epitaxially on the surfaces of ZnO shells, which induces a vertical ZnO nanowires array with the *c*-axis growth direction,



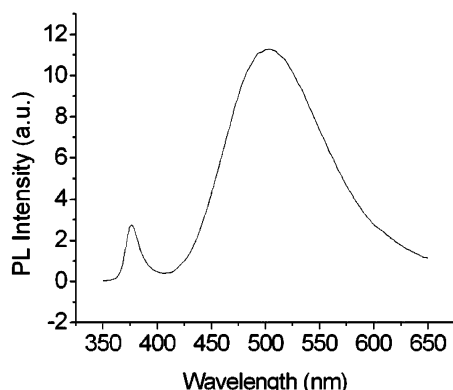


**Figure 6.** Photoluminescence spectrum of ZMBs.

as clearly shown in Figures 1d, 4f, and 5e. The nanowires grow unceasingly, and finally a complete ZnO microberet is formed.

The PL spectra were measured to study the optical properties of ZMBs. Figure 6 shows a weak UV emission centered at 378 nm and a strong broad green emission at around 505 nm. The UV emission peak of ZnO is generally attributed to a recombination of free excitons,<sup>13</sup> and the green emission band is thought to be related to the single ionized oxygen vacancy coming from the recombination of a photogenerated hole with the single ionized charged state of the defect in ZnO.<sup>14</sup> Moreover, it was reported that the oxygen vacancies responsible for the green emission are located at the surface.<sup>15</sup> Therefore, the ratio of UV to green light emission is dependent on the nanostructure's surface area. It is possible that stronger green emission than the UV emission results from an high surface-to-volume ratio of the ZnO microberets. This kind of ZnO microberet with a strong green emission may be used in nanooptoelectronic devices.

A remarkable structural feature of the ZnO microberet is its hollow interior, on which dense nanowires grow vertically on both the inner and outer surfaces of beret shells. This high surface-to-volume ratio of the structure provides a large total surface area, which is desirable as a potential material for solar cell photoanodes. The large surface area will attract more dye loadings onto the surfaces of hollow ZMBs and thus can perform

better light harvesting and greatly improve the light-to-energy conversion efficiency of solar cells.

#### 4. Conclusion

In conclusion, we have synthesized ZMBs by the simple thermal evaporation of Zn powder in the absence of catalyst and template at a relative low temperature (490 °C). In this unique process, ZnO nanowires grow vertically on both the inner and outer surfaces of a microberet shell. The ZMBs possess single-crystalline structure, and their formation basically depends on the optimum starting time of air introduction after the formation of spherical Zn particles. This is a good way to grow well-aligned nanowires by using a nanoscale rough ZnO surface to realize the self-catalyzed VLS process. These types of ZMBs with high surface-to-volume ratios may find potential applications in functional architectural materials, solar cell photoanodes, and nanooptoelectronic devices.

**Acknowledgment.** This work was supported by the National Natural Science Foundation of China (Grant No. 10575078).

#### References and Notes

- (1) Wang, R. C.; Liu, C. P.; Huang, J. L. *Appl. Phys. Lett.* **2005**, *87*, 013110.
- (2) Liao, L.; Li, J. C.; Liu, D. H.; Liu, C.; Wang, D. F.; Song, W. Z.; Fu, Q. *Appl. Phys. Lett.* **2005**, *86*, 083106.
- (3) Könenkamp, R.; Word, R. C.; Schlegel, C. *Appl. Phys. Lett.* **2004**, *85*, 6004.
- (4) Wan, Q.; Li, Q. H.; Chen, Y. J.; Wang, T. H. *Appl. Phys. Lett.* **2004**, *84*, 3654.
- (5) Hughes, W. L.; Wang, Z. L. *Appl. Phys. Lett.* **2003**, *82*, 2886.
- (6) Wang, Z. L. *J. Phys.: Condens. Matter* **2004**, *16*, 829.
- (7) Neves, M. C.; Trindade, T.; Timmons, A. M. B.; Pedrosa de Jesus, J. D. *Mater. Res. Bull.* **2001**, *36*, 1099.
- (8) Kuo, C. L.; Kuo, T. J.; Huang, M. H. *J. Phys. Chem. B* **2005**, *109*, 20115.
- (9) Baxter, J. B.; Aydil, E. S. *Appl. Phys. Lett.* **2005**, *86*, 053114.
- (10) Walsh, D.; Mann, S. *Nature (London)* **1995**, *377*, 320.
- (11) Caruso, F.; Caruso, R. A.; Mohwald, H. *Science* **1998**, *282*, 1111.
- (12) Gao, P. X.; Wang, Z. L. *J. Am. Chem. Soc.* **2003**, *125*, 11299.
- (13) Kong, Y. C.; Yu, D. P.; Zhang, B.; Fang, W.; Feng, S. Q. *Appl. Phys. Lett.* **2001**, *78*, 407.
- (14) Vanheusdan, K.; Warren, W. L.; Seager, C. H.; Tallent, D. R.; Voigt, J. A.; Gnade, B. E. *J. Appl. Phys.* **1996**, *79*, 7983.
- (15) Li, D.; Leung, Y. H.; Djuricic, A. B.; Liu, Z. T.; Xei, M. H.; Shi, S. L.; Xu, S. J.; Chan, W. K. *Appl. Phys. Lett.* **2004**, *85*, 1601.